J. Chem. Sci. (2020)132:87
https://doi.org/10.1007/s12039-020-01798-x

REGULAR ARTICLE

Synthesis, characterization of polystyrene-phosphate films and their application as heterogeneous catalyst for Knoevenagel condensation in solvent-free conditions

HALIMA EL AADAD[a,*], ZAKARIA BENZEKRI[b], SAID BOUKHRIS[b] and ABDELKRIM CHAHINE[a,*]

[a]Laboratory of Physico-Chemistry of Vitreous and Crystallized Materials (LPCVCM), Department of Chemistry, Faculty of Science, Ibn Tofail University, BP 133, 14000 Kenitra, Morocco
[b]Laboratory of Organic Chemistry, Organometallic and Theoretical, Department of Chemistry, Faculty of Sciences, Ibn Tofail University, BP 133, 14000 Kenitra, Morocco
E-mail: halimaelaadad@gmail.com; abdelkrim.chahine@uit.ac.ma

MS received 22 December 2019; revised 30 April 2020; accepted 5 May 2020

Abstract. Novel film catalysts of the polystyrene (Ps) and trimethyl phosphate (P) nanoparticles were synthesized on glass substrates by soft chemistry using doctor blade method. Subsequently, the prepared Ps–P film catalysts were characterized by various techniques, including fourier transform infrared spectroscopy (FTIR), nuclear magnetic resonance (NMR), density (d), polarizing microscope (PM), X-ray diffraction (XRD) and thermal analysis. According to the results, the structure and morphology of film catalysts were confirmed by all analyses. The Ps–P films, as heterogeneous solid catalysts, have demonstrated strong activity for Knoevenagel condensation, producing alkenes of high purity. The recovered yields are excellent, up to 96% in solvent-free conditions at room temperature. Further, the film catalysts have showed high stability, good reusability (up to five times) while maintaining their efficiency and productivity.

Keywords. Film catalyst; doctor blade; heterogeneous catalyst; Knoevenagel condensation; solvent-free.

1. Introduction

The use of polymer materials in film preparation[1] is widely spread across various scientific and technological processes. However, extensive studies have been performed on polymer films using various experimental techniques.[2] Further, the polymer films are increasingly used in many modern technologies and nanotechnologies for: flame retardants,[3] solar cells,[4] optoelectronic,[5] photovoltaic,[6] antibiotic desalination,[7] separation of plant pigments,[8] optical and photoconductive applications.[9] To optimize the use of polymer films, an effective method is desired to improve their stability.[10,11] The stability of the polymer films is related to the interfacial interactions of polymer substrate,[12] thickness of the films, surface heterogeneity and molecular weight of polymers.[13] Therefore, to improve the polymer films stability, many theoretical and experimental studies have been developed for polystyrene films.[14] Moreover, the polystyrene is a material of choice in the filed of sciene and technology,[15–17] due to its favorable properties[18] (transparent, rigid and hard), low cost and easy to process. The introduction of inorganic particles in polystyrene chains is widely used in different technological fields.[19,20] However, these fillers reinforce the polymer matrix by increasing its performance and functionality, which are closely related to the quality of the interface between the organic particles and polymer. Also, among the inorganic particles, those based on phosphate, phosphorus[21,22] is potentially able to form more compounds than carbon. Further, the interest on phosphoric compounds has increased during the last decade for various scientific and technological reasons. According to the studies carried out, these

*For correspondence

Electronic supplementary material: The online version of this article (https://doi.org/10.1007/s12039-020-01798-x) contains supplementary material, which is available to authorized users.

Published online: 23 July 2020

phosphorus compounds have recently shown a major interest in catalysis[23] and photocatalysis.[24]

The Knoevenagel condensation reaction[25] is the most important and useful method in the formation of carbon–carbon bonds by the reaction of carbonyl with activated methylene compounds. Generally, it is catalyzed by a Lewis acid[26] or a homogeneous base[27] in an organic solvent upon heating. Moreover, these catalysts have not solved the Knoevenagel reaction problems, which concern the separation of products, selectivity and reuse of the catalysts. In light of this, there is a strong demand for the improvement of a new catalyst that is free from these problems. According to the above-mentioned considerations, we have synthesized a novel solid heterogeneous catalyst in a film form based on polystyrene–phosphate (Ps–P) which resolves the problems of Knoevenagel reaction.

In this study, new Ps–P film catalysts were synthesized by soft chemistry using doctor blade method[28], and characterized. The structural properties, surface morphology and intermolecular interactions of Ps–P film catalysts were studied with different analysis. The film catalysts are homogeneous, stable, requires 20–60 min for their synthesis and which is carried out in three steps. Moreover, this synthesis is inexpensive and allows energy saving as compared to other catalysts described in the literature. On the other hand, this work presents an invention which evaluates the catalytic activity of film catalysts for the Knoevenagel condensation of different aldehyde derivatives under solvent-free conditions at room temperature. Moreover, it presents an important and convincing industrial utility for the Knoevenagel reaction.

2. Experiment

2.1 *Materials*

The polystyrene $(CH_2\text{-}CH\ (Ph))_n$ (Mw = 250,000) and trimethyl phosphate ($(CH_3)_3PO_4 > 97\%$) were obtained from Acros Organics. The chloroform ($CHCl_3 > 95\%$) was purchased from Prolabo, Fontenay. The polymer and the solvents were used as received. The Ps–P films were deposited on glass substrates. All chemicals of catalytic reaction were purchased from Merck and Fluka Chemical Companies. The known products were identified by comparing their melting points and spectral data with those reported in the literature. The progress of the reaction was monitored by thin-layer chromatography (TLC) using silica gel SIL G/UV254 plates. Melting points were recorded on a Kofler hot stage apparatus and were uncorrected.

2.2 *Preparation of glass substrates and Ps–P film catalysts*

The glass substrates were initially cleaned with a mixture of deionized water and nitric acid (7:3, v/v) for 1 h. Then, they were washed several times with deionized water and dried in an oven. All substrates were cleaned before the preparation of the films.

The Ps–P film catalysts were deposited on glass substrates using doctor blade method (Figure 1). The Ps–P solutions were prepared using different concentrations of trimethyl phosphate in chloroform at room temperature under stirring. Four samples were prepared with different molar ratios R of P/Ps: 0 (F_0), 0.6 (F_1), 1.2 (F_2) and 2.4 (F_3). These solutions were clear and stable, indicating the miscibility and interaction of phosphate with the polystyrene matrix. For the repeatability of results, several tests were performed.

After deposition of the Ps–P films, they were dried in an oven at 60°C and stored under ambient conditions. The thickness of the films was 240 μm and was measured by micrometry.

2.3 *Catalytic activity test of synthesized films*

The Knoevenagel condensation was carried out in different solvents at room temperature (25°C to 30°C) in the absence and presence of the Ps–P film catalyst (m = 0.01 g). The model reaction was the condensation of benzaldehyde-1a (1 mmol) with malononitrile (1 mmol) (Scheme 1) under agitation for appropriate times. After completion of the reaction, dichloromethane was added, stirred for 1 min, then filtered and dried. The resulting solid was recrystallized from absolute ethanol. To seek the optimal conditions of the reaction, we studied the influence of different parameters that control the reaction's evolution, namely: solvent, mass and reuse of the film catalyst.

2.4 *Characterization of Ps–P film catalysts*

2.4a *Fourier transform infrared spectroscopy (FTIR)*: The determination of the Ps–P film catalysts structure and the identification of functional groups were performed using infrared spectroscopy. All infrared spectra were recorded in the 4000-400 cm^{-1} region. The FTIR was performed on a Bruker Tensor 27 spectrometer (Bruker, Germany).

2.4b *Nuclear magnetic resonance spectroscopy (NMR)*: The NMR spectroscopy was performed on a Bruker AVANCE 300 MHz. The ^{13}C-NMR spectroscopy has informed about the distribution of carbon skeletons. The arrangement of hydrogen atoms ^{1}H in the structure of Ps–P film catalysts has been investigated. The ^{31}P-NMR was also studied to show the influence of addition of phosphate on polystyrene matrix.

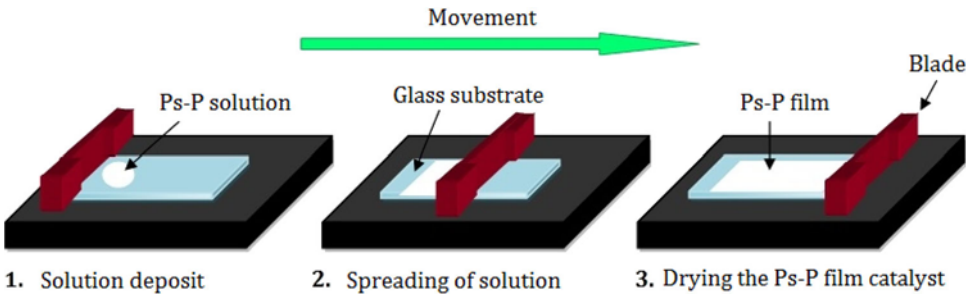

Figure 1. Synthesis of Ps–P film catalysts by doctor blade method.

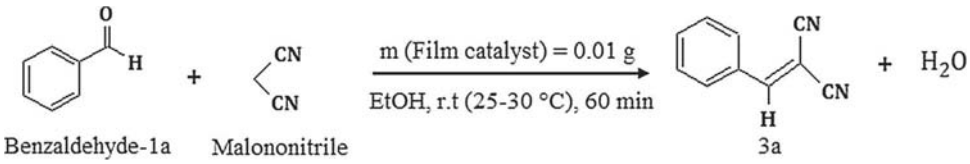

Scheme 1. Knoevenagel condensation reaction in the presence of film catalysts.

2.4c *Density*: The density (d) of Ps–P film catalysts was measured by the pycnometer method[29] at room temperature. The solvent used for this measurement was dimethyl sulfoxide (DMSO). To calculate the density on an adapted balance, we have realized the following three weightings: m_1, pycnometer filled with solvent; m_2, Ps–P film mass + pycnometer filled with solvent; m_3, pycnometer filled with solvent and containing the Ps–P film catalyst.

$$d = \frac{m_2 - m_1}{m_2 - m_3} \times \frac{\rho_{liquid}}{\rho_{water}}.$$

2.4d *The polarizing microscope (PM)*: The surface appearance of the Ps–P film catalysts was carried out by the PM using Leitz Laborlux 11 Pols with a magnification of 50 μm and 20 μm.

2.4e *X-ray diffraction analysis (XRD)*: The structural properties of Ps–P film catalysts were examined by the XRD method using a diffractometer X'Pert[3] Pro MPD PANalytical, with CuKα radiation.

2.4f *Thermal analysis*: Thermal decomposition of Ps–P film catalysts was followed by thermogravimetric analysis (TGA) coupled with differential thermal analysis (DTA). The DTA-TGA was performed on a Labsys provided by SETARAM instrumentation. The heating rate was 10°C/min from 25°C to 600°C.

3. Results and Discussion

3.1 *Fourier transform infrared spectroscopy (FTIR)*

The infrared spectra of the Ps–P film catalysts (F_0, F_1, F_2 and F_3) are shown in Figure 2. The absorption spectrum of the Ps–P film (F_0) showed a set of absorption bands. The broad bands around 3470–3656 cm^{-1} belonged to O–H vibration band.

The absorption bands at 3100–2850 cm^{-1} were assigned to the =C–H stretching vibrations groups and -CH_2- asymmetric stretching vibration of polystyrene.[30] All film catalysts showed the strong peaks at vicinities 1475–1625 cm^{-1} for C=C stretching bonds vibration of aromatic ring.[31] Several characteristic absorption peaks were observed at 760 cm^{-1} corresponding to =CH deformation vibration of aromatic polystyrene bonds.[32]

Moreover, the spectra of the Ps–P film catalysts (F_1, F_2 and F_3) showed new absorption bands in 1300 to 400 cm^{-1} frequency region. A strong band at 1279 cm^{-1} was assigned to P=O stretching vibration.[33,34] The ν_{as} (P–O) stretching vibration appeared at 1184 cm^{-1}. In addition, a broad absorption band at 1043 cm^{-1} was attributed to the ν_{as}(P–O–C) vibration. The peak for ν_s(P–O–C) stretching vibration was observed at 848 cm^{-1}.[35] The δ_{as}(P–O–C) bending was assigned to peak at 450 cm^{-1}.[36] The comparison of the FTIR spectra of pure polystyrene and Ps–P films showed clearly the appearance of new bands corresponding to the interactions of trimethyl phosphate with the polystyrene matrix, and these results were also confirmed by the NMR analysis.

3.2 *Nuclear magnetic resonance spectroscopy (NMR)*

The ^{1}H NMR spectra of pure Ps and Ps–P film catalysts are shown in Figure 3. The small peak at 0.85–0.90 ppm

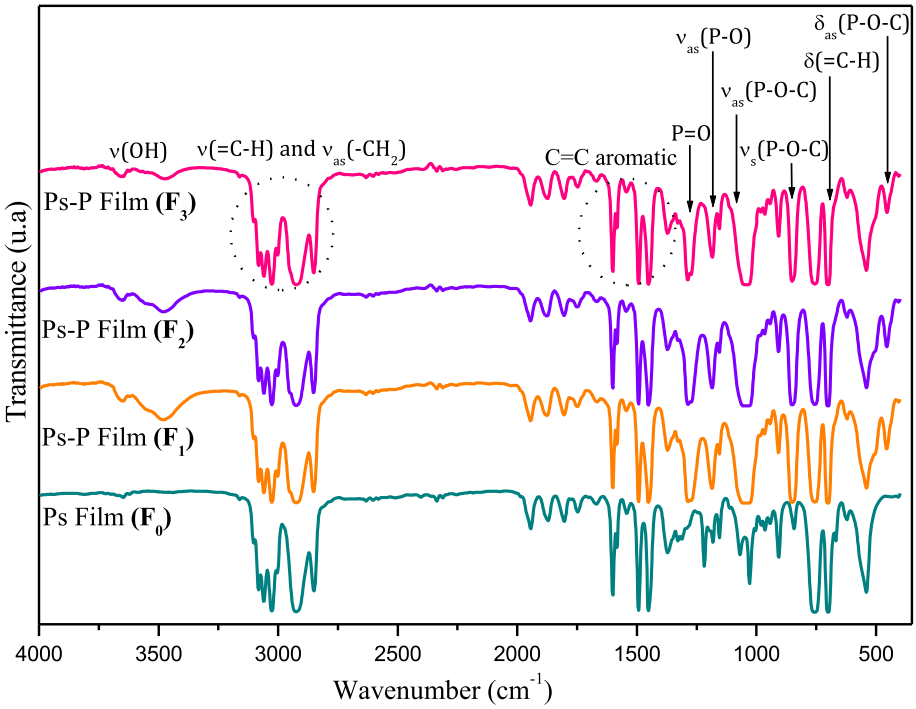

Figure 2. Infrared spectrum of the pure Ps (F_0) and Ps–P film catalysts (F_1, F_2 and F_3).

of pure Ps film **(a)** is assigned to the methyl group of polystyrene (CH_3).[37] All the ^{1}H NMR spectra showed a peak at 5.33 ppm corresponding to CD_2Cl_2 solvent.

The signal appearance at around 1.29 ppm is attributed to CH_2 methyl protons. Moreover, the peak at 1.50–1.74 ppm is ascribed to the CH of polystyrene. A peak observed at 7.07–7.09 ppm is assigned to the characteristic signals of hydrogen of the aromatic benzene ring.

In addition, when trimethyl phosphate was added, we observed the appearance of protons ^{1}H between 3.73–3.77 ppm corresponding to a phosphate,[38] and disappearance of methyl (CH_3) of polystyrene for all the film catalysts (F_1, F_2 and F_3) (Figure 3).[30]

According to the spectral assignments, after the addition of phosphate to the polystyrene matrix, the changes in signal shapes, intensity and difference in the structural organization of the film catalysts can be detected.

As a result, in the ^{13}C NMR spectra (Figure 4), the disappearance of methyl group has been confirmed for all film catalysts F_1, F_2 and F_3. Therefore, this disappearance of methyl group is explained by the formation of P–O–C bonds between the phosphate and polystyrene molecules.

All the ^{13}C NMR spectra showed a peak at 54 ppm in the CD_2Cl_2 solvent. After addition of trimethyl phosphate, the peak (54 ppm) intensity increased, which means that the carbon of trimethyl phosphate appeared in the same signal as CD_2Cl_2.[38]

For the ^{31}P NMR spectra, the signal at 2.24 ppm showed only one peak corresponding to a phosphate group PO_4 of trimethyl phosphate (Figure 5).[39] Indeed, all the film catalysts (F_1, F_2 and F_3) showed a single peak at the same value (2.24 ppm).

3.3 *Density*

The density of pure Ps and Ps–P film catalyst was measured using a pycnometer[40] with DMSO as an immersion liquid. The results showed that the density of Ps–P film catalysts decreased with addition of trimethyl phosphate (Table 1). On one hand, the density depends on the molecular architecture and on the other hand, the main factor determining the density is the mass of the atoms constituting the polymer.[41] It is obvious that more the molecular mass, denser is the polymer. The second factor is the nature of the chemical bonds and their more or less directionality.

According to the results, the decrease in density of film catalysts is probably due to the fact that the molecular architecture of the Ps–P films becomes more ordered after the creation of new bonds between

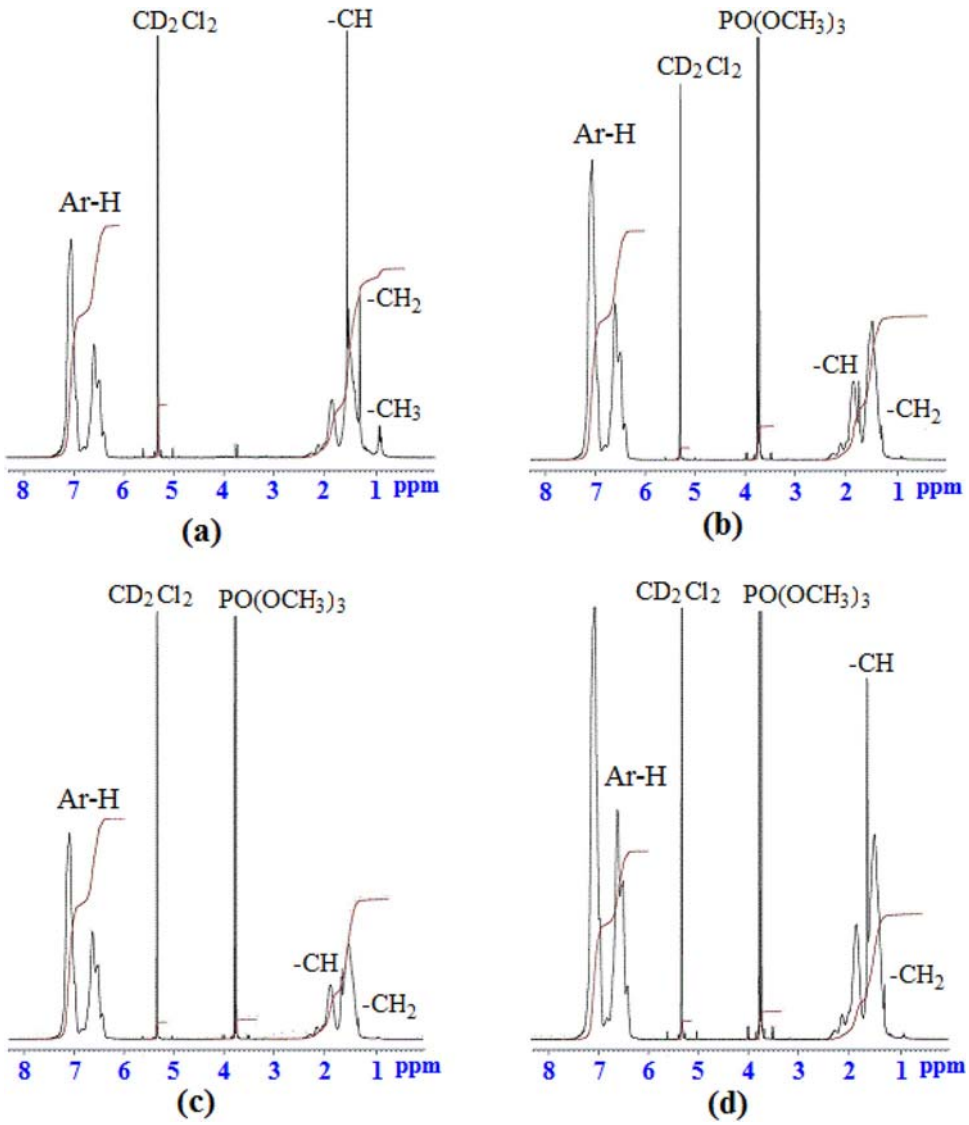

Figure 3. ^{1}H NMR spectra of pure Ps film F_0 (a) and Ps–P film catalysts F_1 (b), F_2 (c) and F_3 (d).

polystyrene and phosphate, which increases the space between the main chains of film catalysts.

3.4 *The polarizing microscope (PM)*

The surface morphology of Ps–P films was studied using a polarizing microscope under ambient conditions. It gives clear images of certain physical properties of the polymer. As shown in Figure 6, the surface of pure Ps film (F_0) shows that the molecular chains are randomly and disorderedly arranged. Further, this image provides information on the amorphous state of the polystyrene and the irregular surface, causing random arrangement of the molecular chains which shows the absence of interactions with the polystyrene molecule.

After the insertion of trimethyl phosphate alkoxide into the polystyrene matrix (F_1, F_2 and F_3), the molecular structure became more orderly and organized (Figure 7).

The surface appearance of the films was relatively smooth and transparent, indicating the great stabilization of polystyrene matrix in the presence of phosphate alkoxide. Therefore, this change confirmed the creation of new chemical bonds between polystyrene and phosphate.

3.5 *X-ray diffraction analysis (XRD)*

The XRD analysis of film catalysts F_0, F_1, F_2 and F_3 are shown in Figure 8. Pure polystyrene is an amorphous material[42] and has no characteristic peak in

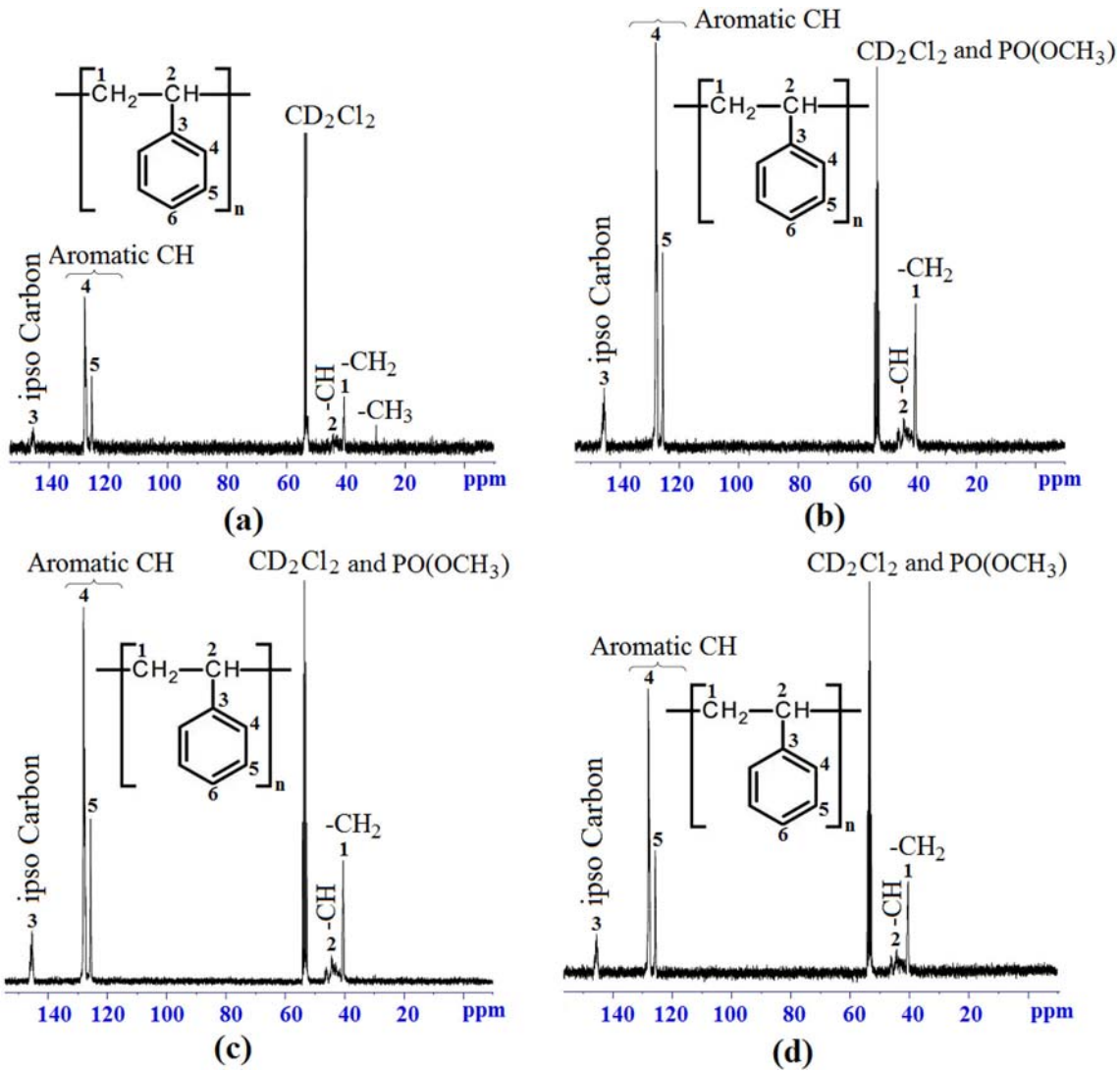

Figure 4. ^{13}C NMR spectra of pure Ps film (a) F_0 and Ps–P film catalysts (b) F_1, (c) F_2 and (d) F_3.

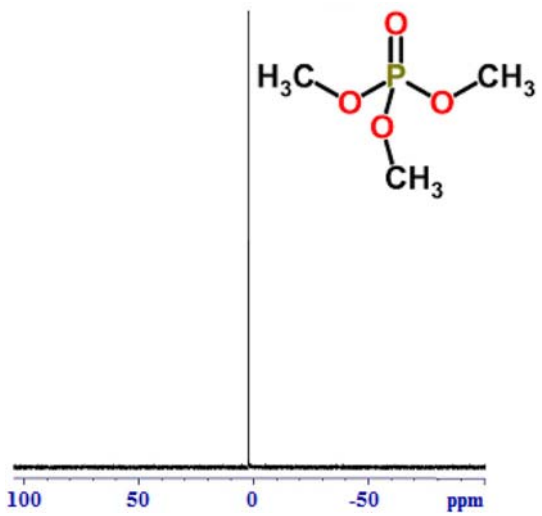

Figure 5. ^{31}P NMR spectra of Ps–P film catalysts (F_1, F_2 and F_3).

Table 1. Density of pure Ps (F_0) and Ps–P (F_1, F_2 and F_3) film catalysts.

Film catalysts	Density
F_0	1.6848
F_1	1.5044
F_2	1.3003
F_3	1.2636

XRD, only two broad peaks (halo) are seen as it has no long-term crystal structure.[43]

As shown in Figure 8, pure Ps and Ps–P films exhibited two broad diffraction peaks[44] located at different diffraction angles 2θ between 9° and 10°, and 19° and 20°. Moreover, the presence of broad peaks in

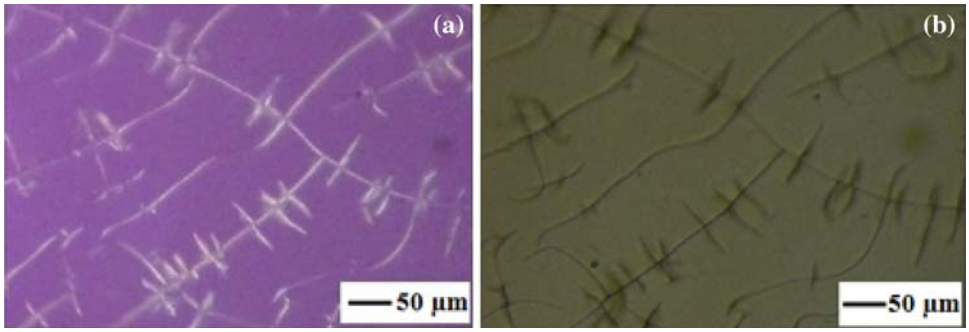

Figure 6. Polarizing microscope images of pure Ps film catalyst. (a) Surface of the Ps film catalyst in polarized light; (b) surface of the Ps film catalyst in natural light.

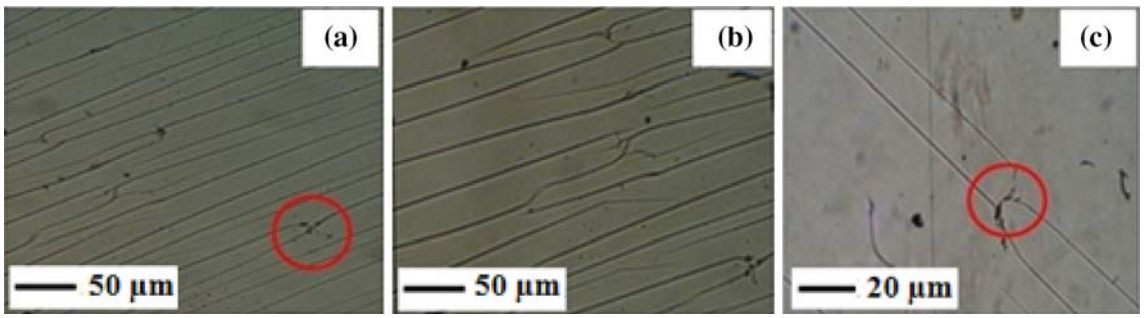

Figure 7. (a) Polarizing microscope images of Ps–P film catalysts. (b) Surface of Ps–P film catalysts in natural light; (c) Surface of Ps–P film catalysts in natural light.

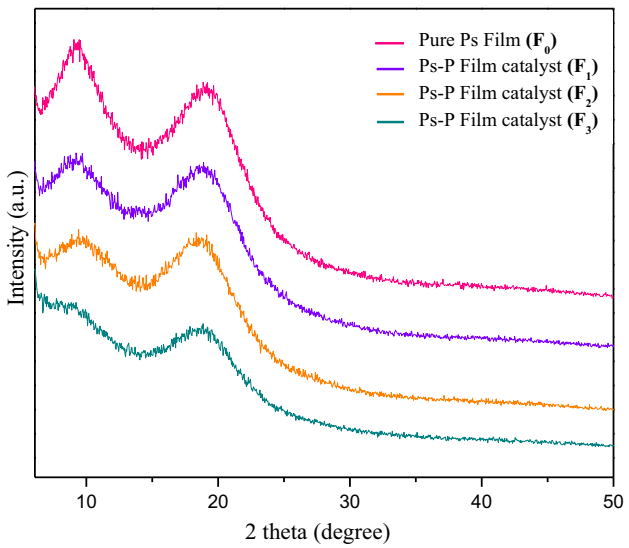

Figure 8. X-ray diffraction patterns of the Ps (F_0) and Ps–P film catalysts (F_1), (F_2) and (F_3).

the XRD patterns of films is an indication of the existence of intermediate range order in these materials.[45] After insertion of trimethyl phosphate in the polystyrene matrix (F_1, F_2 and F_3), the full width at half maximum and peak areas were decreased with increase of phosphate concentration (Table 2).

According to the literature data, the width of the peaks increased with the order of the neighboring main atom, which means that the correlations become increasingly weak. Indeed, in our case, this decrease is due to the correlations between phosphate atoms and polystyrene, which became increasingly strong. Therefore, the effects of the intermolecular interaction of phosphate with polystyrene are predominant.

3.6 *Thermal analysis*

The thermal analysis is an important analytical method in understanding the structure-property relationships and thermal stability of polymers.[46] The polystyrene is thermally degraded into organic compounds such as phenol, quinine and naphthalene at the experimental temperature of 350–450°C.[47] To study the thermal stability of film catalysts, the TG and dTG tests were conducted and is illustrated in Figure 9.

As shown in Figure 9, all the film catalysts F_1, F_2 and F_3 have a higher decomposition temperature T_{dec} than pure polystyrene F_0. The T_{dec} temperature increased with increasing trimethyl phosphate concentration. For all film catalysts, the first stage of weight loss at 133–140°C corresponds to the loss of adsorbed water and organic solvent residues (Figure 9). The pure Ps film (F_0) degraded almost completely (98.7% at 303–425.1°C) (Figure 9a). This

Table 2. X-ray diffraction results of pure Ps (F_0) and Ps–P (F_1, F_2, and F_3) film catalysts.

	Position [°2Th]		Full width and half maximum (°)		Area (a.u.)	
Film catalysts	First peak	Second peak	First peak	Second peak	First peak	Second peak
F_0	9.4654	19.3054	2.9198	3.9801	1889.69	3639.32
F_1 (R = 0.6)	9.4774	19.0501	2.8832	3.8909	1014.50	3052.93
F_2 (R = 1.2)	9.4553	19.0224	2.4233	3.7134	976.32	2093.69
F_3 (R = 2.4)	9.3395	19.0118	1.5984	3.6350	187.58	1725.33

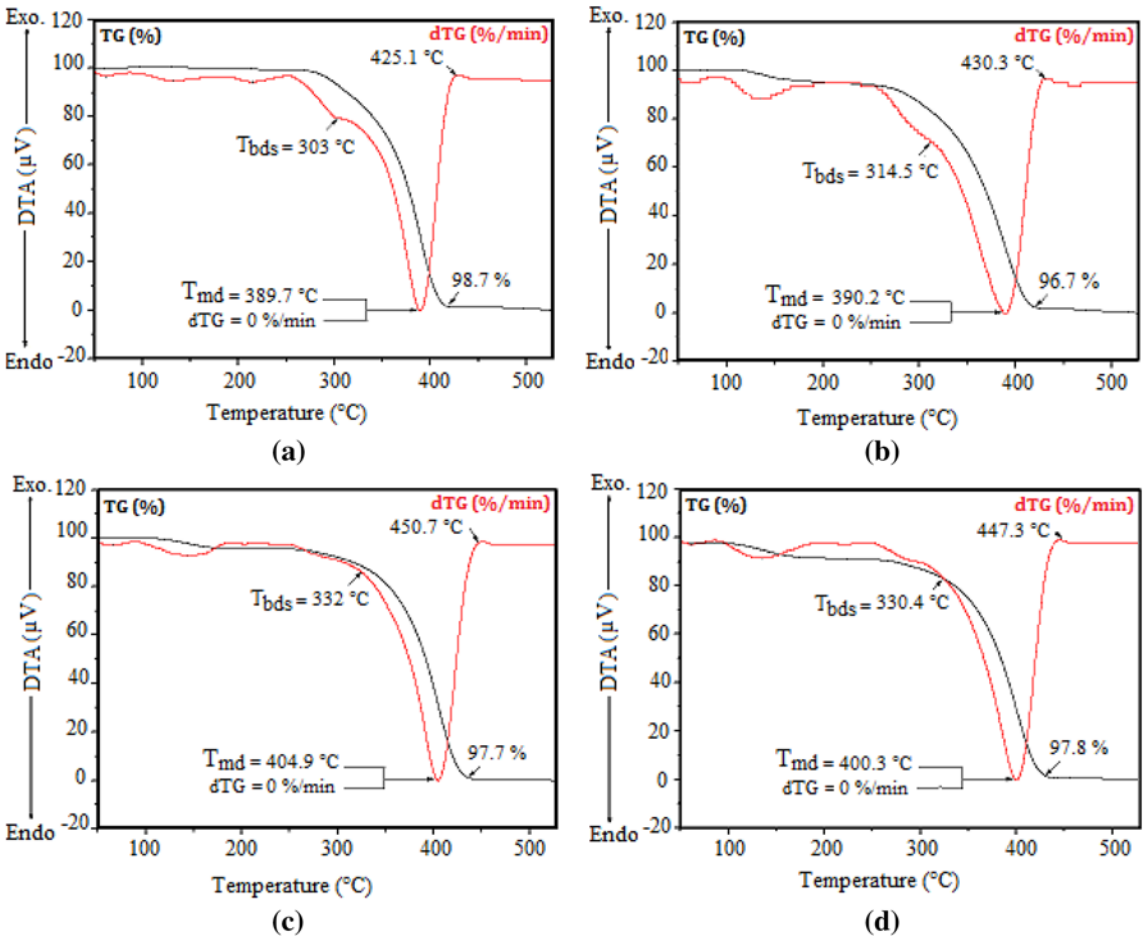

Figure 9. Curves of dTG (%.min^{-1}) and TG (%) of pure Ps and Ps–P film catalysts. (a) Ps film F_0, (b) Ps–P film F_1, (c) Ps–P film F_2, and (d) Ps–P film F_3. Tbds, temperature of brutal degradation start; Tmd, temperature of maximum degradation.

thermal decomposition is mainly due to the depolymerization of the polystyrene molecules. It is accompanied mainly by exothermic energy phenomena.[48]

The weight loss of the film catalyst F_1 (Figure 9b) is particularly noticeable at 150–215.6°C (about 6.5%), and it is due to the reaction between polystyrene and phosphate. The total film weight loss (96.7%) is high at 314–430°C. According to the results of F_2 (Figure 9c) and F_3 film catalysts (Figure 9d), the degradation start temperature is raised to 332°C for the film F_2 and to 330.4°C for the film F_3 and is mainly due to the depolymerization of polystyrene. Further, after the addition of phosphate, the degradation temperature of the polystyrene (97.7%) improved to 332–450.7°C for the film catalyst F_2 and to 330.4–447.3°C for the film F_3, indicating that the presence of phosphate in the polystyrene matrix has

reduced the rate of film catalysts degradation by increasing their thermal stability.[48]

3.7 *Catalytic activity*

The catalytic effect of the synthesized films (F_0, F_1, F_2 and F_3) is tested for the Knoevenagel condensation reaction. Therefore, the reaction of benzaldehyde-1a (1 mmol) with malononitrile (1 mmol) is carried out in ethanol at room temperature for 60 min in the absence and presence of 0.01 g of film catalyst to yield the final product, alkene 3a.

The blank experiment gives the product 3a in only 8% yield. However, in presence of the film catalysts, the yields obtained are 65% for F_0 film catalyst, 90% for F_1, 77% for F_2 and 75% for F_3 (Table 3).

According to our analysis, the most suitable film catalyst for this reaction is F_1 film. To find the optimal conditions of the reaction in presence of F_1 film catalyst, we have studied the influence of catalyst amount and solvent. Reuse of film catalyst was also performed.

3.7a *Effect of the solvent*: Preferably, to study the solvent influence on the chemical reaction and to evaluate the activity of the F_1 film catalyst, we studied the effect of different solvents on the Knoevenagel condensation. The results obtained are shown in Table 4.

The catalytic activity of F_1 film catalyst was remarkably influenced by the solvents. The reaction in EtOH has given the best yield (90%), whereas the reaction in MeOH, butanol, isopropanol and solvent-free has given 85%, 80%, 78% and 80% yields, respectively.

No clear correlation between the solvent polarity and catalytic activity was observed. This result can be attributed to specific interactions between the solvent and the transition state on the one hand and between solvents having one or more heteroatoms on the other hand.

Table 3. Effect of various film catalysts on the condensation Knoevenagel[a].

Entry	Catalyst	Time (min)	Yield[b] (%)
1	–	60	8
2	F_0	60	65
3	**F_1**	**60**	**90**
4	F_2	60	77
5	F_3	60	75

[a]Reaction conditions: benzaldehyde (1 mmol), malononitrile (1 mmol), 0.01 g catalyst, EtOH (3 mL), room temperature (25–30°C), 60 min. Best film catalyst is in bold.
[b]Isolated yield.

Table 4. Optimization of reaction medium for the condensation Knoevenagel[a].

Entry	Solvent	Time (min)	Yield[b] (%)
1	EtOH	60	90
2	MeOH	60	85
3	Butanol	60	80
4	Isopropanol	60	78
5	**Solvent-free**	**60**	**80**

[a]Reaction conditions: benzaldehyde (1 mmol), malononitrile (1 mmol), 0.01 g catalyst, solvent (3 mL), room temperature (25–30°C), 60 min. The interest of the catalyst film in the absence of solvent compared to other solvents is in bold.
[b]Isolated yield.

3.7b *Effect of the mass of F_1 film catalyst in solvent-free conditions*: It is ideal to use this catalyst under the most ecological conditions, namely the reaction without solvent. To determine the possible influence of film catalyst, we carried out the condensation of malononitrile with benzaldehyde using different masses of film catalyst F_1 in solvent-free conditions. The yields obtained after 60 min of the reaction at room temperature (25–30°C) are shown in Figure 10.

It shows clearly that the yield of product and the catalytic activity were remarkably influenced by the amount of catalyst. Interestingly, the yield of 3a product was significantly increased to 84% by using 0.17 mol % (0.018 g) of catalyst.

3.7c *Reuse of F_1 film catalyst*: The study of film catalyst reuse is an important step in catalysis. For this, the reuse of F_1 film catalyst in Knoevenagel reaction is studied under optimal conditions (F_1 with a mass of 0.018 g, solvent-free). The results are shown in Figure 11. The present catalyst can be used up to five times while maintaining its efficiency and productivity.

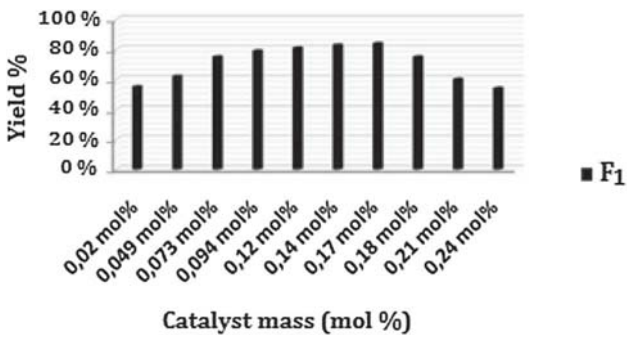

Figure 10. Effect of the F_1 film catalyst mass on the Knoevenagel reaction yield.

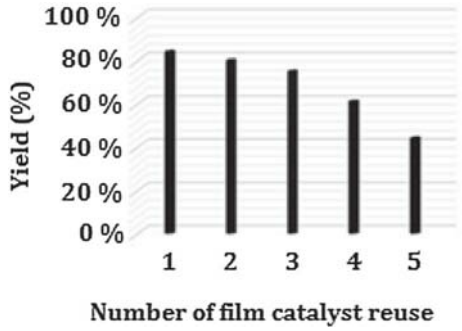

Figure 11. The reuse of F_1 film catalyst in Knoevenagel condensation reaction.

3.7d *Catalytic activity of F_1 film for the synthesis of other alkenes*: We have previously defined the optimal conditions for catalysis of Knoevenagel reaction (model). To test the catalytic activity of F_1 film catalyst, we studied its catalytic capacity for the synthesis of other alkenes. The method consists of carrying out the condensation of activated malononitrile on aldehydes as a function of time to determine the ideal time for the formation of each alkene (Scheme 2).

The obtained results are shown in Table 5.[49] From these results, we find that the reaction times vary according to the nature of the aromatic aldehydes.

The F_1 film catalyst has shown that it is a good catalyst for Knoevenagel condensation of aromatic aldehydes with malononitrile. The obtained yields are greater than 84% (84% for R = H, 94% for R = –Cl, 96% for R = –Me and 94% for R = $–NO_2$). Further, these film catalysts have several advantages: the solid state of films makes them easily reusable, the composition contains no toxic products, and the absence of solvent in the catalysis reactions is environment friendly. The characteristics of new film catalyst (yield, mass, reaction time, reuse, absence of solvent and simplicity of isolation) make it easily usable in the industry.

3.7e *Evaluation of catalytic activity of F_1 film catalyst with the earlier reported systems*: To demonstrate the merits of our work, it seemed interesting and necessary to compare our results for the synthesis of **3a-d** products by Knoevenagel condensation in the presence of **F_1** film catalyst compared with some other catalysts cited in the literature.

The comparison of **F_1** film catalyst efficiency with other reported catalyst for the present reaction is given in Table 6.

The results shown in Table 6 reveal that the catalytic capacity of our **F_1** film catalyst is more efficient and it has some advantages than those reported in the literature in terms of shorter reaction time, low mass of film catalyst, high yields in solvent-free and in ambient conditions. Moreover, our catalyst is inexpensive, nontoxic, effective, easy to handle and to recover, and it acts both as catalyst and as support.

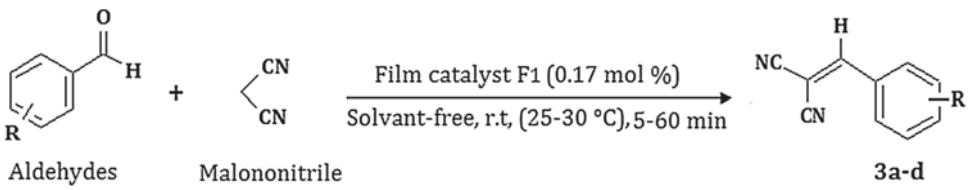

Scheme 2. Synthesis of alkenes 3a-d in the presence of F_1 film catalyst R = H, -Cl, -Me, $-NO_2$.

Table 5. Solvent-free condensation of Knoevenagel reaction in presence of F_1 film catalyst.

Entry	R	Ar	Time (min)[a]	Yield[b] (%)	Melting point (°C)	
					Found	Reported
3a	H	C_6H_5	60	84	80–81	80–81[49]
3b	-Cl	*p*-ClC_6H_4	6	94	158–159	159–160[49]
3c	-Me	*p*-MeC_6H_4	9	96	118–119	118–120[49]
3d	$-NO_2$	*p*-$NO_2C_6H_4$	5	94	161–162	160–161[49]

[a]Time reported in min monitored by TLC. [b]Isolated yields.

Table 6. Comparison of catalytic activity of the F_1 film catalyst for the Knoevenagel condensation with other reported compounds.

Catalyst	Reaction conditions	Time	Yield (%)	Reference
CAU-1-NH_2	Aldehyde (1 mmol), malononitrile (1 mmol), catalyst (0.025 g), EtOH, 40°C	7 h	80–91	50
([$Zn(Py_2TTz)(2\text{-}NH_2\text{-}BDC)$]·$(DMF))_n$	Aldehyde (1 mmol), malononitrile (2 mmol), catalyst (0.02 mol), solvent-free, 60°C	6 h	89–99.9	51
$Ni_2(pca)_2(H_2O)_6{\cdot}2H_2O$	Aldehyde (1 mmol), malononitrile (1 mmol), catalyst (6 mol %), solvent-free, 50°C	5 h	80–97	52
Zn-Bp-BTC	Aldehyde (1 equi), malononitrile (1.1 equi), catalyst (0.06 mol), MeOH, 60°C	3 h	99	53
Chitosan	Aldehyde (1 mmol), malononitrile (1 mmol), catalyst (0.025 g), EtOH, 40°C	1 h	85–98	54
$[Cd_3(tipp)(bpdc)_2]{\cdot}DMA{\cdot}9H_2O$	Aldehyde (1 mmol), malononitrile (2 mmol), catalyst (0.006 mmol), solvent-free, 60°C	1 h	91–99	55
ZrKP-MePh	Aldehyde (1 mmol), malononitrile (1 mmol), catalyst (2 mol %), solvent-free, Rt	1 h	94–96	56
$K_{11}H[P_2W_{18}O_{68}(HOSn^{IV}OH)_3].20H_2O$	Aldehyde (1 mmol), malononitrile (1.2 mmol), catalyst (0.010 g), EtOH, Rt	20–80 min	90–95	57
CdO + $[CdNa_2\ (\mu\text{-}L^2)]n.6.34\ H_2O$	Aldehyde (1 mmol), malononitrile (1 mmol), catalyst (0.15 + 0.01 mol), solvent-free, Rt	20 min	88	58
n-Fe_3O_4/PVAm nanocomposite	Aldehyde (1 mmol), malononitrile (1 mmol), catalyst (0.030 g), Solvent-free, 40°C	10 min	98.6	59
Clay A, PC-A	Aldehyde (2 mmol), malononitrile (2 mmol), catalyst (0.1 g), EtOH/H_2O, 40°C	5–12 min	98	60
Film catalyst F_1	**Aldehyde (1 mmol), malononitrile (1 mmol), catalyst (0.018 g)(0.17 mol %), solvent-free, Rt**	**5 min–1 h**	**84–96**	**This work**

Rt, room temperature.

4. Conclusion

In the present work, the Ps–P film catalysts have been successfully prepared on glass substrates by soft chemistry route using the doctor blade method. The structure and properties of the prepared film catalysts were characterized using FTIR, NMR, density, PM, XRD and TG-DTA analyses. The catalytic activities of these film catalysts were studied for Knoevenagel condensation and the film catalyst F_1 was selected for detailed study.

The F_1 film has demonstrated an excellent catalytic activity (up to 96%) for Knoevenagel condensation in solvent-free conditions. Indeed, we have established a solid heterogeneous catalyst, effective, non-toxic, inexpensive, easily usable, and reusable up to five times. This study also highlights the great potential of F_1 film catalyst for a suitable industrial application.

Supplementary Information (SI)

The color, melting point, ^1H NMR and ^{13}C NMR spectra of all synthesized products by Knoevenagel condensation reaction in presence of film catalysts are available at www.ias.ac.in/chemsci.

Acknowledgements

We thank Dr Mrabet Souad for their assistance in the polarizing microscope analysis.

References

1. Luo R, Li H, Du B, Zhou S and Zhu Y 2020 A simple strategy for high stretchable, flexible and conductive polymer films based on PEDOT: PSS-PDMS blends *Org. Electron.* **76** 105451
2. Karim A and Kumar S 2000 In *Polymer surfaces, interfaces and thin films* (World Scientific Publishing Company) p. 304
3. Yin X, Zhang Z, Wu M, Zhang J and Xu G 2018 Toward transparent composite films with selective solar spectral, flame retardant and thermal insulation functions *Mater. Chem. Phys.* **216** 365
4. Mohammed M I, El-sadek M S A and Yahia I S 2020 Optical linearity and bandgap analysis of RhB-doped PMMA/FTO polymeric composites films: a new designed optical system for laser power attenuation *Opt. Laser Technol.* **121** 105823
5. Bathula C, Khadtare S, Buruga K, Kadam A, Shrestha N K and Noh Y 2018 Selenophene based benzodithiophene polymers as potential candidates for optoelectronic applications *Dye. Pigment.* **149** 639
6. Rafique S, Abdullah S M, Badiei N, McGettrick J, Lai K T, Roslan N A, Lee H K H, Tsoi W C and Li L 2019 An insight into the air stability of the benchmark polymer: Fullerene photovoltaic films and devices: A comparative study *Org. Electron.* **76** 105456
7. Wang Z, Guo S, Zhang B and Zhu L 2019 Hydrophilic polymers of intrinsic microporosity as water transport nanochannels of highly permeable thin-film nanocomposite membranes used for antibiotic desalination *J. Memb. Sci.* **592** 117375
8. Ismayil K M M, Manaf O, Sujith A and Antony R 2019 Polymer thin films for chromatographic separation of plant pigments *Mater. Lett.* **252** 321
9. Ali F M, Ashraf I M and Alqahtani S M 2017 Promising Cu-doped polyvinyl alcohol films for optical and photoconductive applications *Phys. B Condens. Matter* **527** 24
10. Pangpaiboon N, Traiphol N, Promarak V and Traiphol R 2013 Retardation the dewetting dynamics of ultrathin polystyrene films using highly branched aromatic molecules as additives *Thin Solid Films* **548** 323
11. Oluwaleye O, Madhuku M, Mwakikunga B and Moloi S J 2019 Studies of lattice structure, electrical properties, thermal and chemical stability of cobalt ion implanted Indium Tin Oxide (ITO) thin films on polymer substrates *Nucl. Instruments Methods Phys. Res. Sect. B Beam Interact. Mater. Atoms* **450** 267
12. Xue L and Han Y 2011 Pattern formation by dewetting of polymer thin film. *Prog. Polym. Sci.* **36** 269
13. Li Z, Zhong W, Ying L, Liu F, Li N, Huang F and Cao Y 2019 Morphology optimization via molecular weight tuning of donor polymer enables all-polymer solar cells with simultaneously improved performance and stability *Nano Energy* **64** 103931
14. Arinda P S, Santjojo D J D H, Masruroh M and Sakti S P 2019 Stability of polystyrene film surface wettability modified using oxygen plasma *Mater. Today Proc.* **13** 24
15. Mouhamad Y, Mokarian-Tabari P, Jones R A L and Geoghegan M 2019 Application of mean-field theory to the spin casting of polystyrene and poly (methyl methacrylate) blend films from toluene *Polymer* **178** 121578
16. Das S and Mahalingam H 2019 Dye degradation studies using immobilized pristine and waste polystyrene-TiO_2/rGO/g-C3N4 nanocomposite photocatalytic film in a novel airlift reactor under solar light *J. Environ. Chem. Eng.* **7** 103289
17. Jalal N M, Jabur A R, Hamza M S and Allami S 2019 Preparation, microstructure and morphology of electrospun sulfonated polystyrene films for proton exchange membrane hydrogen fuel cell *Energy Proc.* **157** 1494
18. Sabet M, Soleimani H, Mohammadian E and Hosseini S 2019 Impact of inclusion graphene oxide nanosheets on polystyrene properties *Int. J. Plas. Technol.*1–9
19. Bhavsar S, Patel G B and Singh N L 2018 Investigation of optical properties of aluminium oxide doped polystyrene polymer nanocomposite films *Phys. B Condens. Matter* **533** 12
20. James J, Unni A B, Taleb K, Chapel J P, Kalarikkal N, Varghese S, Vignaud G and Grohens Y 2019 Surface engineering of polystyrene–cerium oxide nanocomposite thin films for refractive index enhancement *Nano-Struct. Nano-Obj.* **17** 34
21. Chouryal Y N, Sharma R K, Acharjee D Gnguly T, Pandey A and Ghosh P 2019 Influence of ionic liquids and concentration of red phosphorous on luminescent Cu_3P nanocrystals *J. Chem. Sci.* **131** 93
22. El Aadad H, Rair D and Chahine A 2019 Synthesis and characterization of novel organic–inorganic hybrid nanocomposites of phosphate–benzimidazole by soft chemistry route in aqueous media *SN Appl. Sci.* **1** 1474
23. Mncwabe Z, Farahani M D and Friedrich H B 2019 Switching between oxidation types using molybdenum phosphate catalysts for paraffin activation using doped fe as surface acidity modifier and MoO x as an oxygen insertion tool *Catal. Lett.* 1
24. Omer K M, Mohammad N N and Baban S O 2018 Upconversion fluorescence of phosphorous and nitrogen co-doped carbon quantum dots (CDs) coupled with weak LED light source for full-spectrum driven photocatalytic degradation via ZnO-CDs nanocomposites *Catal. Lett.* **148** 2746
25. Jadhav A L and Yadav G D 2019 Clean synthesis of benzylidenemalononitrile by Knoevenagel condensation of benzaldehyde and malononitrile: effect of combustion fuel on activity and selectivity of Ti-hydrotalcite and Zn-hydrotalcite catalysts *J. Chem. Sci.* **131** 79
26. Prajapati D, Lekhok K C, Sandhu J S and Ghosh A C 1996 Lithium bromide as a new catalyst for carbon–carbon bond formation in the solid state *J. Chem. Soc. Perkin Trans.* **9** 959
27. Brufola G, Fringuelli F, Piermatti O and Ferdinando P 1997 Efficient one-pot synthesis of 7-azacoumarins by Knoevenagel reaction using water as reaction medium *Heterocycles.* **45** 1715
28. Berni A, Mennig M and Schmidt H 2004 Doctor blade In *Sol-gel technologies for glass producers and users* p.89
29. Degallaix S and Ilschner B 2007 In *Caractérisation expérimentale des matériaux I (TM volume 2) Propriétés physiques, thermiques et mécaniques* in (ed. Presses Polytechniques Et Universitaires Romandes) p.420

30. Biémont É 2008 In *Spectroscopie moléculaire, Structures moléculaires et analyse spectrale* in (ed. De Boeck supérieur) p.320
31. Branan N and Wells T A 2007 Microorganism characterization using ATR–FTIR on an ultrathin polystyrene layer *Vib. Spectrosc.* **44** 192
32. Rair D, El aadad H, Jermoumi T and Chahine A 2018 Spectroscopic and thermal degradation studies of novel hybrid polymer based on sodium polyphosphate - polystyrene *Med. J. Chem.* **7** 337
33. Tekin N and Cebe M 2004 Solvents effect on infrared spectra of trimethyl phosphate in organic solvents *Vib. Spectrosc.* **36** 129
34. Reva I, Simao A and Fausto R 2005 Conformational properties of trimethyl phosphate monomer *Chem. Phys. Lett.* **406** 126
35. Mäkie P, Westin G, Persson P and Österlund L 2011 Adsorption of trimethyl phosphate on maghemite hematite, and goethite nanoparticles *J. Phys. Chem. A* **115** 8948
36. Mastrantonio G and Della Védova C O 2001 Spectroscopic and conformational comparative study of trimethyl chalcogenphosphates *J. Mol. Struct.* **561** 161
37. Bevington J C and Huckerby T N 2006 Studies of end-groups in polystyrene using 1H NMR *Eur. Polym. J.* **42** 1433
38. Streck R and Barnes A J 1999 Solvent effects on infrared, 13C and 31P NMR spectra of trimethyl phosphate: Part 1. Single solvent systems *Spectrochim. Acta Part A Mol. Biomol. Spectrosc.* **55** 1049
39. Meng Q, Doetschman D C, Rizos A K, Lee M H, Schulte J T, Spyros A and Kanyi C W 2011 Adsorption of organophosphates into microporous and mesoporous NaX zeolites and subsequent chemistry *Environ. Sci. Technol.* **45** 3000
40. OCDE 2012 Ligne directrice de l'OCDE pour les essais de produits chimiques. Daphnia magna, essai de reproduction *OECD Environ. Heal. Saf. Publ.* p.28
41. Belitskus D 1993 In *Fiber and whisker reinforced ceramics for structural applications.* in (ed. CRC Press) p.11
42. Alekseeva O V, Bagrovskaya N A and Noskov A V 2018 Effect of C60 filling on structure and properties of composite films based on polystyrene *Arab. J. Chem.* **11** 1160
43. Botan R, Nogueira T R, Lona L M F and Wypych F 2011 Synthesis and characterization of exfoliated polystyrene-layered double hydroxide nanocomposites via in situ polymerization. *Polímeros-Ciência e Tecnol.* **21** 34
44. Bhadra J, Al-Thani N J, Madi N K and Al-Maadeed M A 2013 Preparation and characterization of chemically synthesized polyaniline–polystyrene blends as a carbon dioxide gas sensor *Synth. Met.* **181** 27
45. N'Dri K, Houphouet-Boigny D and Jumas J C 2012 Study of first sharp diffraction peak in As_2S_3 glasses by X-ray powder diffraction method *J. Non-Oxide Glas.* **3** 29
46. Ahmetli G, Cerit A and Kocaman S 2013 Synthesis and characterization of UV-crosslinkable unsaturated ketone group containing polystyrene films *Prog. Org. Coat.* **76** 884
47. Faravelli T, Bozzano G, Colombo M, Ranzi E and Dente M 2003 Kinetic modeling of the thermal degradation of polyethylene and polystyrene mixtures *J. Anal. Appl. Pyrolysis* **70** 761
48. El Watik L, Antonetti P, Claire Y, Zineddine H, Kaloustian J, Rossi C and Perichaud A. 1998 Etude de la dégradation thermique du polystyrène choc ignifugé *J. Therm. Anal. Calorim.* **53** 297
49. Benzekri Z, El Mejdoubi K, Boukhris S, Sallek B, Lakhrissi B and Souizi A 2016 Dicalcium phosphate dehydrate DCPD as a highly efficient and reusable catalyst for Knoevenagel condensation *Synth. Commun.* **46** 442
50. Dhakshinamoorthy A, Heidenreich N, Lenzen D and Stock N 2017 Knoevenagel condensation reaction catalysed by Al-MOFs with CAU-1 and CAU-10-type structures *Cryst. Eng. Comm.* **19** 4187
51. Zhai Z W, Yang S H, Lv Y R, Du C X, Li L K and Zang S Q 2019 Amino functionalized Zn/Cd-metal–organic frameworks for selective CO_2 adsorption and Knoevenagel condensation reactions *Dalt. Trans.* **48** 4007
52. Rong N, Qiu T, Qian R, Lü L, Huang X, Ma Z and Cui C 2017 Three pyrazole-3-carboxylic acid complexes as efficient solvent-free heterogeneous catalysts for CC bond formation *Inorg. Chem. Commun.* **86** 98
53. Madasamy K, Kumaraguru S, Sankar V, Mannathan S and Kathiresan M A 2019 Zn based metal organic framework as a heterogeneous catalyst for C–C bond formation reactions *New J. Chem.* **43** 3793
54. Sakthivel B and Dhakshinamoorthy A 2017 Chitosan as a reusable solid base catalyst for Knoevenagel condensation reaction *J. Colloid Interface Sci.* **485** 75
55. Jiang W, Yang J, Liu Y-Y, Song S-Y and Ma J-F 2017 A stable porphyrin-based porous mog metal–organic framework as an efficient solvent-free catalyst for C–C bond formation *Inorg. Chem.* **56** 3036
56. Rosati O, Lanari D, Scavo R, Persia D, Marmottini F, Nocchetti M, Curini M and Piermatti O 2018 Zirconium potassium phosphate methyl and/or phenyl phosphonates as heterogeneous catalysts for Knoevenagel condensation under solvent free conditions *Microporous Mesoporous Mater.* **268** 251
57. Khoshnavazi R, Bahrami L and Rezaei M 2017 Heteropolytungstostannate as a homo-and heterogeneous catalyst for Knoevenagel condensations, selective oxidation of sulfides and oxidative amination of aldehydes *RSC Adv.* **7** 45495
58. Jlassi R, Ribeiro A P, Tiago G A, Wang J, Krawczyk M S, Martins L M D R S, Naili H, Pombeiro A J L and Rekik W 2018 Elementary and efficient catalyst process for the Knoevenagel condensation of araldehydes with arylmethylidene malononitrile *Inorg. Chim. Acta* **471** 76
59. Arghan M, Koukabi N and Kolvari E 2019 Polyvinyl amine as a modified and grafted shell for Fe_3O_4 nanoparticles: As a strong solid base catalyst for the synthesis of various dihydropyrano [2, 3-c] pyrazole derivatives and the Knoevenagel condensation *J. Saudi Chem. Soc.* **23** 150
60. Ouaddari H, Beqqour D, Bennazha J, El Amrani I E, Albizane A, Solhy A and Varma R S 2018 Natural Moroccan clays: Comparative study of their application as recyclable catalysts in Knoevenagel condensation *Sustain. Chem. Pharm.* **10** 1